Spectroscopic study of the detachment phases in the W-7AS stellarator with island divertors

U. Wenzel, K. McCormick, N. Ramasubramanian,
F. Gadelmeier, P. Grigull, R. König, H. Thomsen
Max-Planck-Institut für Plasmaphysik, Euratom Association,
D-85748 Garching, Germany

1 Abstract

We give an experimental overview of the detachment process in the W7-AS stellarator with island divertors. Results of different spectroscopic methods are combined with the neutral pressure measurements. We find two phases of the detachment process: the detachment transition triggered by a thermal instability and a volume recombination phase for densities well above the detachment limit. The first phase is characterized by a sudden drop of the temperature at the plasma edge and in the divertor. As a consequence the particle fluxes at the divertor targets on top and at bottom are reduced in some regions. In the second phase a strong carbon radiation belt has developed inboard midplane so that the divertor plasma cools down up to the onset of volume recombination only in the upper divertors.

2 Introduction

Wendelstein 7-AS (R=2m, $a_{eff} \leq 0.16m$ and $B_t \leq 2.5T$) is a modular, low shear stellarator with 5 magnetic field periods. Over one period the plasma shape varies from a standing ellipse to a triangle and back again. Depending on the rotational transform ι_a the plasma is bounded either by a smooth surface or by a separatrix formed from natural magnetic islands. The island divertor concept makes use of these islands for particle and energy removal. The five divertor module pairs (top-bottom) follow the magnetic islands in the ι=5/9 configuration. They cut the region around the elliptical plane with a length of about 0.7 m covering about 25% of the toroidal circumference.

The installation of the island divertor allowed access to a new operation regime. In the high density H-mode (HDH) very high line-averaged densities (up to $4 \cdot 10^{20} m^{-3}$) were quasi- stationary obtained over many energy confinement times [1]. As a consequence the electron densities in the divertor are also high, although a non-linear increase due to the flux amplification like in tokamaks was not observed. The reason is the high importance of cross-field diffusion due to the small field line pitch of the island divertors. Despite the absence of the high recycling regime, a roll-over and a subsequent decrease of the particle fluxes to the target plates was found when increasing the density. The decrease was observed by the Langmuir probes and the H_α diagnostic.

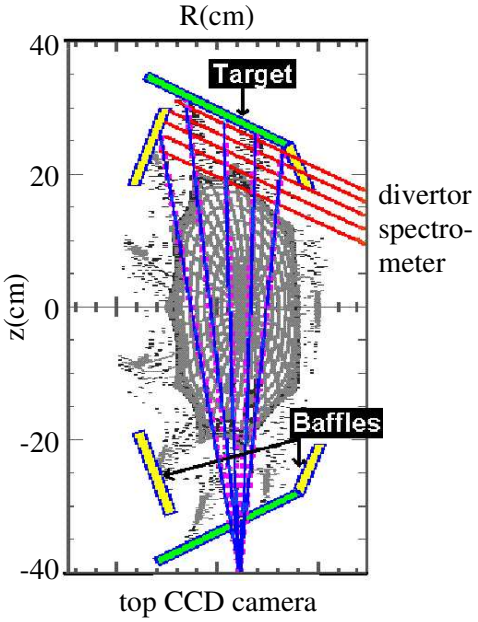

Figure 1: Poloidal cross-section of Wendelstein 7-AS showing the divertor targets and baffles. The upper divertor is observed by a CCD camera with interference filters and by a divertor spectrometer with lines-of-sight nearly parallel to the target plate.

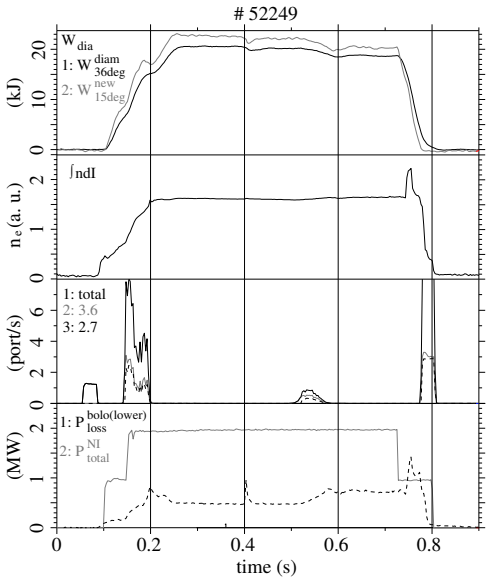

Figure 2: Time traces of shot #52249: energy content, line-averaged density, gas flux, neutral beam injection and total radiated power (broken line). From 0.5 s the density rises by the gas puff triggering the detachment transition at 0.55 s.

3 The detachment transition

The diagnostic of the island divertor is concentrated in the modules (at bottom) and 2 (on top). Fig. 1 shows a poloidal cross-section of W7-AS with the divertor targets. They are arranged to cut the two magnetic islands on top and at bottom in the $\iota = 5/9$ configuration. The plasma in the upper divertor is observed by a CCD camera with an interference filter and by a spectrometer with lines-of-sight parallel to the target plate. The divertor at bottom is studied by a system of three CCD cameras allowing the simultaneous observation at three wavelengths. The neutral pressure is measured both in the upper and lower sub-divertor range by ionization manometers [2]. Furthermore, optical signals are sampled from the midplane to characterize the plasma edge out of the divertor.

Fig. 2 shows the time traces of shot #52249. The energy content of the discharge is 20kJ. Neutral beam power amounts to 2MW. The line-averaged density ($n_e = 2.6 \cdot 10^{20} m^{-2}$) is very close to the detachment threshold. From 0.5 s on the density rises by the gas puff up to $n_e = 2.7 \cdot 10^{20} m^{-2}$. By the small density rise the total radiated power also increases. Above a definite radiation level the divertor plasma detaches.

To determine the transition point we look for correlations between optical signals from midplane and the sub-divertor neutral pressures (Fig. 3). The midplane signals sample the edge radiation of hydrogen (H_α) and carbon (CIII at $\lambda = 465\,nm$). The CIII

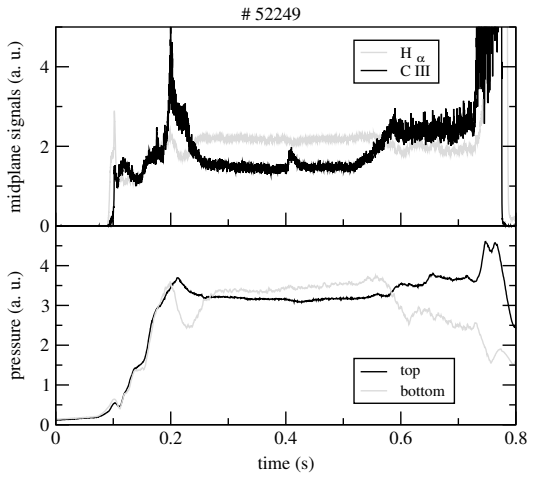

Figure 3: Optical signals from midplane (up) and sub-divertor neutral pressures from the upper and lower divertor regions (down). The carbon radiation starts to increase at t=0.52 s triggering the detachment transition at t=0.55 s as evident by the decay of H_α in the midplane and the sub-divertor neutral pressure at bottom.

signal rises with the density. It is correlated with the increase of the total radiated power (Fig. 2). At the detachment transition at 0.55 s the H_α emission decreases while the CIII continues to rise. When the plasma detaches, the sub-divertor drops in the lower divertor (Fig. 3). The pressure drop in the lower divertor is correlated with the decrease of the H_α signal at midplane. Therefore, we consider the point at t = 0.55s as the detachment transition.

The detachment transition is characterized by the following observations: 1) decrease of the temperature at midplane 2) detachment of the carbon radiation from the target plate and 3) drop of the particle flux in the divertor.

We show here as an example the detachment of the carbon emission in the upper divertor. The signals were sampled by the divertor spectrometer having lines-of-sight nearly parallel to the divertor plates. Fig. 4 shows the spatial distributions of CIII ($\lambda = 465\,nm$) for the relevant time range between 0.45 and 0.65 s. In the attached phase the maximum of the CIII radiation is located 20mm away from the target plate. At t=0.55 s the maximum emission starts to shift away from the plate. The radiation zone stabilizes at a position x=40mm at t=0.6s. How do we interpret the shift of the carbon emission zone? For the production and excitation of the CIII ion a typical energy of 7 eV is necessary [3]. This means that the CIII ion will emit at the position where the temperature is about 7eV. With other words, the detached position of the CIII radiation corresponds to the position of the 7eV contour. Attached means that the temperature at the target plate is greater than 7 eV; in this case the CIII ion will always exist near the target plate. From the movement of the CIII emission we conclude, that at the detachment transition the temperature in the upper divertor drops below 7 eV.

4 Detached divertor plasma with volume recombination

Increasing the density further after the detachment transition results in a new phase of the detachment process. The plasma cools down up to the onset of volume recombination. This phase is characterized by the following experimental observations: 1) strong carbon emission from the inboard side (midplane), 2) up-down asymmetry of the sub-divertor

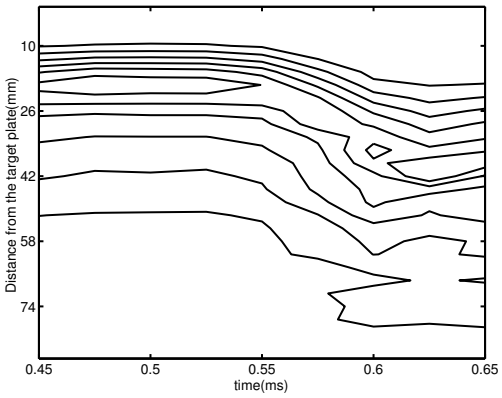

Figure 4: Lines of equal CIII intensities in the upper divertor module measured by the divertor spectrometer. At the transition point at t=0.55 s the CIII emission zone detaches from the target plate. This indicates a drop of the temperature below 7 eV.

neutral pressure and 3) strong H_β emission in front of the upper target. These features are shown in the following subsections.

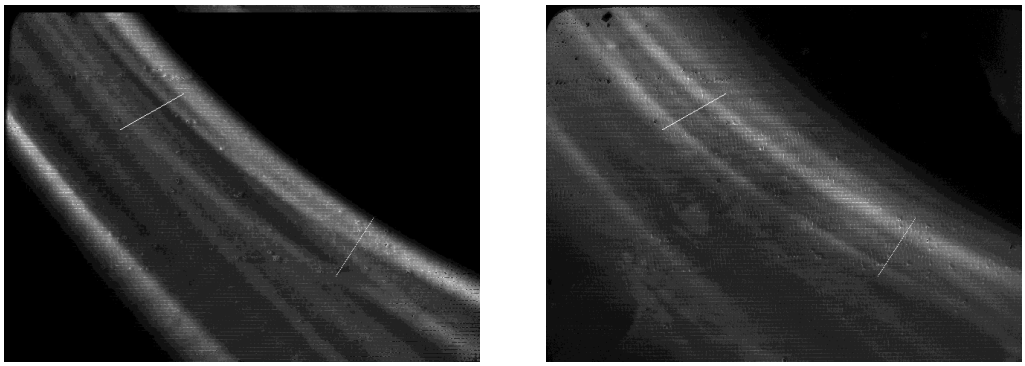

Figure 5: View of the divertor plasma at bottom of a detached discharge with volume recombination: H_α (right) and CIII (left). Data is taken at t=0.45s of the deeply detached shot #56244. Target tiles 5 and 13 are indicated by the white lines. The H_α picture shows two strike lines which is the typical pattern of a detached discharge. However, the CIII emission is dominated by a radiation belt from inboard. The strike line pattern is much weaker pronounced in the light of CIII than this zone.

4.1 Strong carbon emission from the inboard side

Fig. 5 shows CCD camera pictures of the divertor plasma at bottom taken with an H_α and a CIII ($\lambda = 465\,nm$) filter (shot #56244 at t=0.45s). The H_α picture exhibits the two strike lines without the double structure which is the typical pattern in a detached discharge. In the CIII picture the corresponding strike lines are also visible. However, the most intense part of the radiation does not originate from the plasma target interaction but from the inboard side. The strike lines are only weakly pronounced. The radiation belt is absent or at least very weak in the H_α emission. The stripe left down in the CIII picture is an extension from the upper divertor module either from the divertor or from the inboard side. Since the radiative losses are mainly due to the carbon ions CIII and CIV we conclude that the main radiation in the deeply detached state comes no longer from the divertor region but from the edge plasma at the inboard position.

4.2 Large up-down asymmetry of the sub-divertor neutral pressure

Fig. 6 shows the optical signals (CIII and H_α) from midplane and the sub-divertor neutral pressures. The CIII intensity increases in two steps at t=0.15 s and t=0.18 s. At the latter time the sub-divertor neutral pressure at bottom stagnates. This correlation defines the detachment transition.

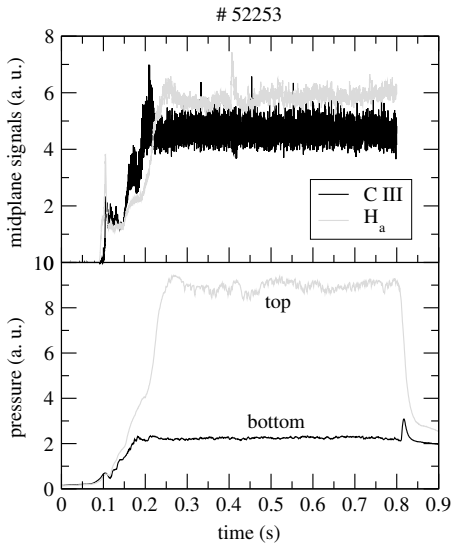

Figure 6: Optical signals from midplane (upper plot) and sub-divertor neutral pressures from the upper and lower divertor regions (lower plot). Data is from shot #52253. The rise of CIII from the midplane is due to the detachment. Later a large sub-divertor neutral pressure up/down asymmetry develops which indicates a new phase in the detachment.

Fig. 6 shows that the H_α signal from midplane does not react when the divertor plasma detaches. It rises at later time (t=0.2 s) when the CIII intensity is already constant. The rise of the H_α midplane signal defines a second phase in the detachment process in which also the sub-divertor neutral pressure strongly rises in the upper divertor. Since the pressure in the divertor at bottom stagnates, a large up/down asymmetry is the consequence.

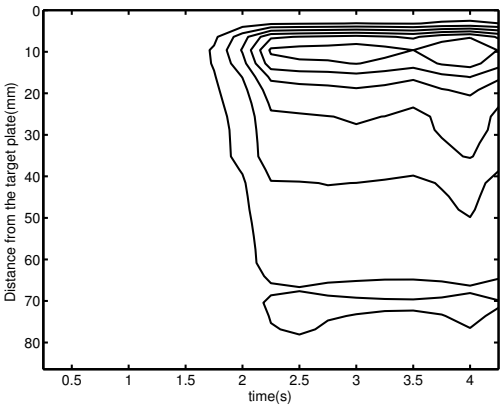

Figure 7: Lines of equal H_β intensity in the upper divertor module measured by the divertor spectrometer (shot #52253). The strong increase of the H_β radiation in front of the target is due to volume recombination.

4.3 Strong H_β emission in front of the upper target

Fig. 7 shows the line emission of hydrogen (H_β) when the new phase of the detachement process is observed. At 2.0s the H_β radiation strongly rises near the target plate. This

rise is always correlated with a pronounced Balmer spectrum near the series limit which is due to three-body recombination. The temperature for the transition from an ionizing to recombining plasma is about 1.3 eV. We conclude that in the second phase a low temperature region near the target has formed in which the plasma recombines.

5 Summary

We studied the detachment process in the W7-AS stellarator with island divertors by spectroscopic and neutral pressure diagnostics. The detachment occurs in two phases: the detachment transition and the onset of significant volume recombination in the upper divertor at higher densities. In the first phase, the plasma edge becomes thermally unstable below a certain edge temperature. As a consequence, the temperature in the edge plasma drops. This drop was experimentally detected in the divertor and at midplane. The thermal instability is connected with the radiative loss function of carbon, i.e. it occurs for $T_e \approx 30eV$. In the second phase a strong radiation belt has formed at inboard position which dominates even over the divertor radiation. It is only visible in the light of CIII but not in H_α. From this finding we exclude the formation of a Marfe which is a condensation phenomenon on closed flux surfaces. Marfes were observed in W7-AS at still higher densities also in the light of H_α [4]. Due to the high radiative losses some parts in the upper divertor with high tile numbers cool down to about 1eV so that volume recombination sets in. The physical mechanism is three-body recombination which becomes very efficient for low T_e and high n_e.

References

[1] K. McCormick, P. Grigull, R. Burhenn, et al., A New Advanced Operational Regime on the W7-AS Stellerator, Phys. Rev. Lett. **89**, 015001 (2002).

[2] K. McCormcick, P. Grigull, H. Ehmler, et al., Neutral compression in the W7-AS stellarator divertor, in *Europhysics Conference Abstracts (CD-ROM), Proc. of the 2001 EPS Conference on Controlled Fusion and Plasma Physics, Madeira, 2001*, volume 25A, page 2105, 2001.

[3] U. Wenzel, A. Carlson, C. Fuchs, et al., Spectroscopic Study of the Radiation in Divertor I of ASDEX Upgrade at High Density, Plasma Phys. Controlled Fusion **41**(6), 801–818 (1999).

[4] U. Wenzel, K. McCormick, D. Hildebrandt, et al., Experimental observation of Marfes in the W7-AS stellerator, Plasma Phys. Controlled Fusion **44**, L57–L62 (2002).